CONF-
790125--63

DEFECT PRODUCTION AND ELECTRONIC STOPPING FOR LIGHT IONS IN METALS

by

R.S. Averback, R. Benedek, K.L. Merkle and L.J. Thompson

MASTER

Prepared for

Fusion Reactor Materials Conference

Miami Beach, Florida

January 29-31, 1979

U of C-AUA-USDOE

ARGONNE NATIONAL LABORATORY, ARGONNE, ILLINOIS

Operated under Contract W-31-109-Eng-38 for the

U. S. DEPARTMENT OF ENERGY

DEFECT PRODUCTION AND ELECTRONIC STOPPING FOR LIGHT IONS IN METALS*

R. S. AVERBACK, R. BENEDEK, K. L. MERKLE, AND L. J. THOMPSON

Materials Science Division, Argonne National Laboratory, Argonne, Illinois 60439

A method for determining effective electronic stopping powers in metals is presented. The method involves measuring damage rates in thin films as a function of ion energy. The experimental results are compared with predictions based on Monte Carlo computer simulations. Results are presented for H, D, He, and Li projectiles on Cu, Ag, and Ni. The implication of these results for defect production is discussed.

1. INTRODUCTION

The implantation of light gas atoms into first-wall materials can have many adverse effects on fusion reactors. Helium implantation, for example, causes erosion of metals by sputtering and blistering. Gas retention and release by the first wall can also affect reactor performance. To predict these radiation effects and to evaluate their significance for reactor design, it is necessary to obtain a theoretical understanding of such basic characteristics of the ion-solid interaction as electronic stopping powers, range and damage distributions, and defect production.

Recent work in our laboratory has been directed toward developing an understanding of the basic defect-production processes in metals. For light-ion irradiations, accurate values for the electronic stopping are required to calculate defect production. This can be seen from the following relation [1,2] for the number of Frenkel pairs produced by an ion of incident energy E:

$$\nu^t(E) = \int \frac{dE'}{S_n(E')+S_e(E')} \int dT \, \frac{d\sigma(T,E')}{dT} \, \nu(T). \quad (1)$$

Here $S_n(E')$ and $S_e(E')$ are the nuclear and electronic stopping cross sections, respectively; $d\sigma(T,E')/dT$ is the scattering cross section for an ion of energy E' to produce a host-atom recoil of energy T; and $\nu(T)$ is the number of Frenkel pairs produced by a recoil of energy T. For light-ion irradiations, $S_e(E) >> S_n(E)$. This paper deals with a new semiempirical method of determining $S_e(E)$. The implications of our results for defect-production calculations are also discussed.

The most usual and direct method of determining stopping powers in solids is to measure the energy loss in the undeflected portion of an ion beam that passes through a thin-film specimen. The application of this "direct" approach to low-energy ions, however, has been difficult. For these measurements, extremely thin specimens are required. It is difficult, however, to control and accurately characterize the thickness, uniformity and possible surface contamination of such specimens. In addition, multiple scattering of the ions complicates the analysis [3]. Finally, one may question the validity of deriving stopping powers from measurements on only the undeflected portion of the beam. Few of these ions undergo small impact-parameter collisions, and the energy-loss characteristics of the measured beam may not be representative of a more random set of trajectories.

As an alternative to the "direct" approach, stopping powers have been deduced from projectile range distributions. This method has the advantage of not requiring ultrathin specimens, and gives equal weight to all trajectories. However, it has been used primarily with very high implantation doses, and at temperatures at which the implanted ions can diffuse. These conditions may alter the final distribution of implanted ions from their true range distribution.

In this paper, we present a method to determine effective electronic stopping powers from damage-rate measurements in thin metal films. This technique is analogous to deriving stopping powers from range measurements, but large implantation doses are not required and diffusion of defects is suppressed. Information about defect-production distributions produced by low-energy ions is also important in understanding radiation effects in first-wall materials. This follows from the strong interaction of implanted gas with vacancies and vacancy clusters [4]. Copper, silver and nickel were selected as targets in this work. A large amount of data regarding stopping powers and ranges for light ions in these metals is available for comparison [5,6].

2. METHOD

The number of Frenkel pairs produced by an ion incident on a metal film can be deduced from the equation

$$\nu^e = \frac{N_o t}{\rho_F} \frac{d\Delta\rho}{d\phi} \quad . \quad (2)$$

Here N_o is the atomic concentration,
t is the specimen thickness,
ρ_F is the Frenkel pair resistivity,
$\Delta\rho$ is the radiation-induced resistivity increment,
and ϕ is the ion dose.

*Work supported by the U. S. Department of Energy.

The use and validity of eq. (2) are described elsewhere [2]. Damage rates were measured at 6 K for a series of ion energies. As the beam energy is varied the defect-production distribution is changed within the specimen as schematically illustrated in fig. 1. The damage

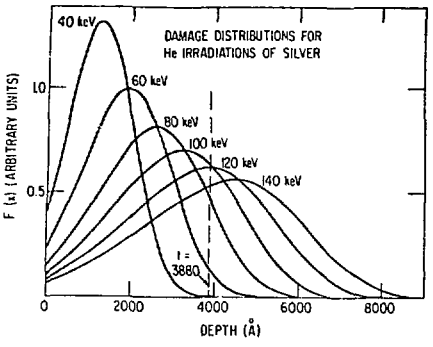

Fig. 1. Damage distributions for He irradiations of silver.

rate, $d\Delta\rho/d\phi$, is proportional to the integral of the defect-production distribution between the two specimen surfaces. Based on fig. 1, it is apparent that $\nu^e(E,t)$ should initially rise with increasing energy, reach a maximum, and then decrease. This behavior is observed experimentally, as shown in fig. 2 (lower curve).

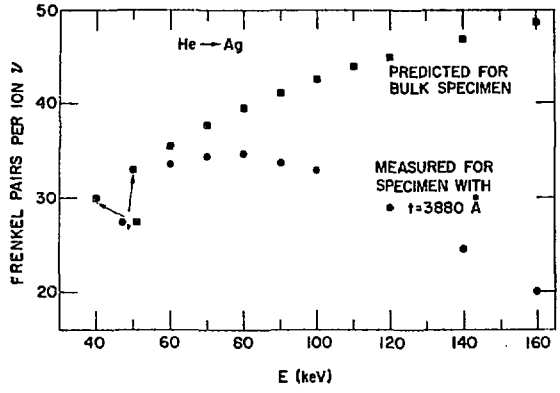

Fig. 2. Frenkel-pair production versus irradiation energy for He irradiation of silver.

The exact energy dependence of $\nu^e(E,t)$ is a sensitive function of the stopping power.

The upper curve in fig. 2 is a semiempirical estimate of the Frenkel-pair production for a semiinfinite specimen, $\nu^e(E,\infty)$. The curve was generated from the relationship

$$\nu^e(E,\infty) = \nu^t(E)\xi(E) , \qquad (3)$$

where $\nu^t(E)$ is the defect production calculated according to eq. (1) and $\xi(E)$ is an efficiency (or normalization) factor. The efficiency factor relates the true defect production to the defect production calculated from eq. (1). For the 40-keV He irradiation of the silver specimen shown in fig. 2, essentially all of the ions are stopped within the specimens and $\nu^e(E,t) = \nu^e(E,\infty)$. From this equality and eq. (3), we find $\xi(40\ \text{keV})=0.62$. The factor $\xi(E)$ varies slowly with energy (by ~10% over the energy intervals covered by the present irradiations [2]). This rather small variation of $\xi(E)$ is a consequence of the insensitivity of the primary recoil spectrum to ion energy; i.e., the Frenkel pairs created by a 40- or 100-keV He irradiation are produced by host-atom recoils of similar energy. In the present work $\xi(E)$ has been estimated from ref. 2. The reflection of energy from the front surface of the specimen is not included in eq. (1). Both experiment [7] and computer simulation show, however, that the energy reflection is less than a few percent for the present irradiations.

The deviation of $\nu^e(E,t)$ from $\nu^e(E,\infty)$ at high energies in fig. 2 is attributed to the transmission of a portion of the beam energy through the back surface of the foil. This energy would create additional defects in a (hypothetical) bulk specimen. We define the ratio of $\nu^e(E,t)$ to $\nu(E,\infty)$ as the "containment fraction":

$$\alpha(E,t) \equiv \nu^e(E,t)/\nu^e(E,\infty) . \qquad (4)$$

In principle, a defect-production distribution could be derived from these measurements by obtaining $\alpha(E,t)$ as a function of t (i.e., several specimens) and fixed E, and then taking the derivative $d\alpha(E,t)/dt$ as a function of t. It is far simpler and more accurate to obtain the containment fraction as a function of E with fixed t (i.e., one specimen). This type of profile can be related to the theory in the same way as the usual damage distribution. We have, therefore, adopted this procedure. The stopping power is deduced by generating theoretical curves for $\alpha(E,t)$ with the stopping as a parameter and comparing these curves to the experimental $\alpha(E,t)$ function.

We have used the Monte Carlo computer simulation TRIM [8] to generate the theoretical containment-fraction profiles. The TRIM code was modified slightly in order to obtain the defect-production profile instead of the damage-energy profile. This was accomplished by assigning $\nu^t(T)$ Frenkel pairs to each host-atom recoil of energy T, where $\nu^t(T)$ is the same modified Kinchin-Pease form of the damage function as employed in ref. 2 and eq. (1).

3. EXPERIMENTAL PROCEDURE

The experimental details involved in measuring damage rates of thin-film specimens at low temperatures have been described elsewhere [2]. Only a few essential details are mentioned here. The specimens were polycrystalline films grown by vapor deposition onto rock salt. The specimen thicknesses (~3000 Å) were determined by measuring the weight gain of monitor foils adjacent to the specimens. For each evaporation, ten sets of specimens and five monitor foils were obtained. The monitor foils showed thickness variations of ~5%; we consider the uncertainty in the thickness determination to be of

this magnitude. The specimens were mounted in the cryostat with the film normal tilted ~10° from the axis to minimize texture effects.

For the thin, pure specimens employed in the present experiments, there is a size effect on the electrical resistivity. The procedure for obtaining the absolute size-effect correction is described elsewhere [2,9]. To obtain containment-fraction profiles, only relative damage rates are necessary. In analyzing the data, however, it is necessary to correct for changes in the size effect and radiation annealing since each damage-rate measurement involves a small but finite resistivity increment, ~$1 \times 10^{-9}\Omega$-cm. This correction can be made rather accurately by repeating the damage-rate measurement at a fixed energy several times during the irradiation sequence [2,10]. The damage rate at this energy serves to normalize the damage rates at all other energies.

4. RESULTS

Figures (3-8) show experimental and theoretical $\alpha(E,t)$ curves for several of the ion-target combinations examined. The experimental curves were determined from the data using eqs. (1) and (2); the theoretical curves are the results of TRIM. The form of the electronic stopping employed by TRIM is

$$S_e(E) = \frac{S_L \cdot S_B}{S_L + S_B} \qquad (5)$$

where S_L and S_B are the Lindhard-Scharff [11] and Bethe [12] expressions, respectively. For all irradiations in this work except those using the highest-energy protons, eq. (5) essentially reduces to the Lindhard-Scharff relation,

$$S_L = kE^{1/2} . \qquad (6)$$

The value of the electronic stopping coefficient k is treated as a parameter in TRIM. In each figure, values of k are specified in units of k_L, the value obtained from the formula of Lindhard and Scharff [11]. The theoretical curves fit the experimental curves reasonably well for a unique value of k. In most cases, however, there is a small increase in the effective value of k, $k_{eff}(E)$, with an increase in energy. Moreover, this effect appears to become more pronounced with increasing projec-

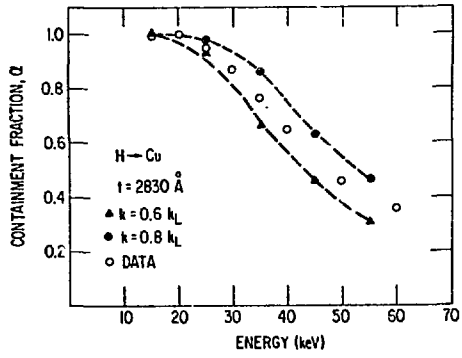

Fig. 3. Containment fraction versus energy for H irradiation of copper.

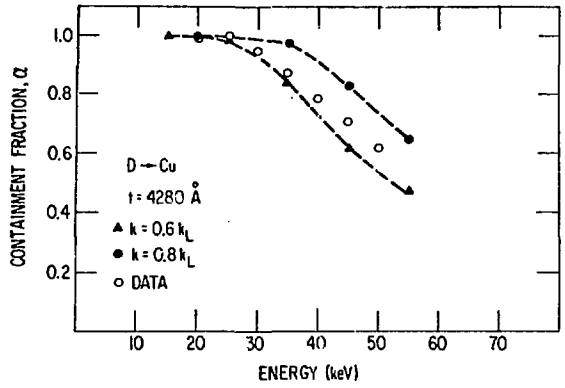

Fig. 4. Containment fraction versus energy for D irradiation of copper.

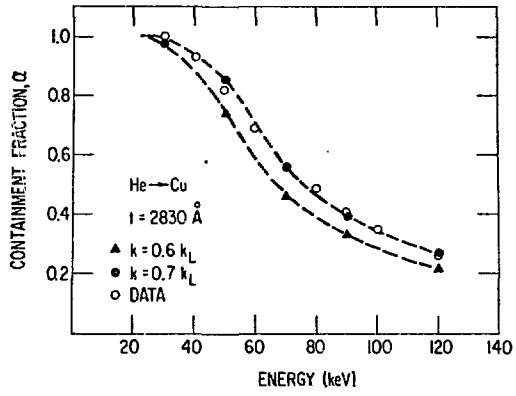

Fig. 5. Containment fraction versus energy for He irradiation of copper.

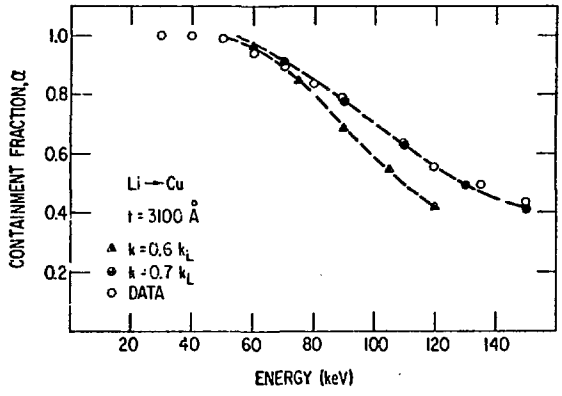

Fig. 6. Containment fraction versus energy for Li irradiation of copper.

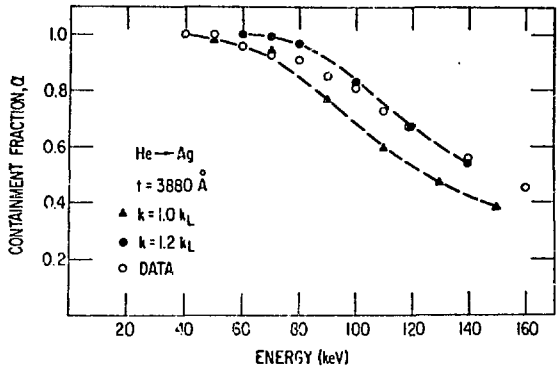

Fig. 7. Containment fraction versus energy for He irradiation of silver.

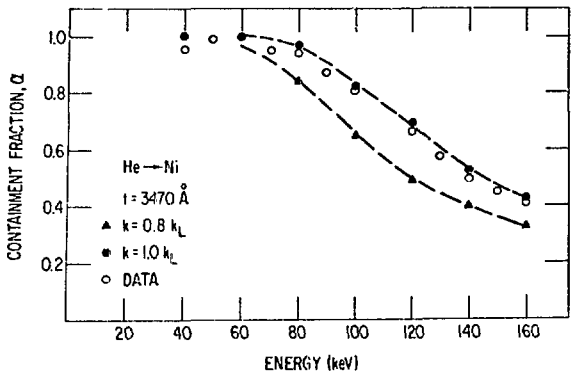

Fig. 8. Containment fraction versus energy for He irradiation of nickel.

tile mass. In any case, the function $\kappa_{eff}(E)$ does not vary more than ∿10% from the mean value of $k_{eff}(E)$.

The electronic stopping coefficients for all of the ion-target combinations examined are shown in Table 1. These values correspond to the value of k for which the theoretical and experimental curves intersect at $\alpha(E,t) = 0.5$. At this energy, the thickness of the specimen, t, is the mean damage depth for the distribution in an infinite medium. This criterion for selecting k was adopted to minimize the effect of "tails" in the distribution and also to maximize the sensitivity of the results to the electronic stopping. This procedure is analogous to using the mean range of the incident ions to derive the electronic stopping.

A direct comparison of the present results with previous data based on energy-loss methods should be regarded with caution. The effective stopping coefficient $k_{eff}(E)$ is determined by the stopping power at all energies of the projectile along its trajectory within the specimen. Therefore $k_{eff}E^{1/2}$ cannot be regarded as the stopping power at energy E unless eq. 6 holds exactly. Nevertheless, the values for k derived from "best fit" curves in Refs. 5 and 6 (hereafter referred to as A-Z) are listed in

Table 1

Electronic Stopping Coefficient for Several Ion-Target Combinations

Target	Ion	Thickness	E_c[a] (keV)	k/k_L[b]	$k(A-Z)/k_L$[b]
Copper	H	2830	45	0.7	1.05
	D	4280	50	0.7	1.05
	He	2830	70	0.7	1.00
	He	3100	85	0.7	1.00
	He	4280	120	0.7	1.00
	Li	2830	100	0.7	—
	Li	3100	120	0.7	—
Silver	H	2640	50	1.15	1.6
	D	2640	40	1.2	1.6
	He	2640	85	1.2	1.5
	He	3880	140	1.2	1.5
	Li	3880	200	1.2	—
Nickel	He	3470	140	0.95	1.15

a) Energy of incident ion for which $\alpha(E,t)=0.5$.
b) k_L is the value of k obtained from the Lindhard-Scharff formula [11].

Table 1 for comparison. The present results are lower than the A-Z values by ∿30% for all cases. It should be pointed out, however, that considerable scatter exists within the data base from which the A-Z values were derived. Some of those data agree very well with the present results. It is interesting to note that for both copper and silver targets, the relative stopping values obtained for H and He in the present work are the same as those of A-Z. Moreover, there is agreement between the A-Z values and our values for the relative stopping in copper and silver for each projectile.

The importance of accurate electronic stopping values for defect-production calculations is seen in Table 2. The number of Frenkel pairs produced by an ion of incident energy E, $\nu^e(E)$, is listed for various light-ion irradiations of copper and silver. The ratio, ξ [eq. (3)], between experimental and theoretical values is also shown, The efficiencies are listed for three choices of the stopping power: the Lindhard-Scharff values, the A-Z values, and the presently reported values. It can be seen that ξ is nearly proportional to the assumed value of k. The decrease of ξ with increasing projectile mass has been attributed to the sensitivity of the primary recoil spectrum to projectile mass [1,2].

5. DISCUSSION

Two general questions arise regarding the validity of our method for deriving effective stopping powers: first, does the analysis of the resistivity measurements [eqs. (2) and (3)] yield correct experimental values for the containment fraction α; second, do the Monte Carlo

Table 2

Defect Production by Light Ions

Target	Ion	E_o[a] (keV)	ν^e	ξ	ξ(A-Z)	ξ(L)
Copper	H	20	7.8	0.86	1.25	1.2
	D	20	21.4	0.87	1.24	1.18
	He	30	63	0.775	1.00	1.00
	Li	40	127.3	0.76		0.94
Silver	H	20	2.8	0.87	1.19	0.76
	D	15	7.1	0.83	1.08	0.70
	He	40	29.9	0.72	0.87	0.62
	Li	40	55.1	0.65		0.58

calculations provide a sufficiently accurate simulation of the ion trajectories? In connection with the first point, one may question the validity of eq. (2) in the presence of a non-homogeneous defect distribution. This matter is discussed in detail in Ref. 2, in which several experimental tests that support the use of eq. (2) are reported. In the context of the present work, the agreement between the results for the stopping in specimens of different thicknesses is encouraging.

The theoretical analysis is based on the assumption of an amorphous target. Although care was taken in the experiments to prevent channeling of the incident beam, some channeling may be unavoidable for the low-energy projectiles employed in this work. This behavior would extend the ranges of the projectiles, and our analyses would consequently underestimate the stopping power. Transmission sputtering experiments, which also provide information on damage distributions, do show extended "tails" in the damage distribution for a 50-keV He irradiation of gold [13]. These tails are not predicted by theories which employ the amorphous-target assumption. If crystallinity effects are important, this may explain some of the discrepancy between the present results and the A-Z values, which are based on energy-loss measurements.

REFERENCES

[1] R. S. Averback, R. Benedek, and K. L. Merkle, App. Phys. Letts. 30, (1977) 455.

[2] R. S. Averback, R. Benedek and K. L. Merkle, Phys. Rev. B., 18, (1978) 4156.

[3] L. Meyer, Phys. Stat. Sol. 44, (1971) 253.

[4] W. D. Wilson, M. I. Baskes, and C. L. Bisson, Phys. Rev. B13, (1976) 2470.

[5] H. H. Andersen and J. F. Ziegler, Hydrogen, Stopping Powers and Ranges on All Elements (Pergamon Press, New York, 1977).

[6] J. F. Ziegler, Helium, Electronic Stopping Powers and Ranges in All Elemental Matter (Pergamon Press, New York, 1977).

[7] H. H. Andersen, T. Lenskjaer, G. Sidenius and H. Sorensen, J. Appl. Phys. 47, (1976) 13.

[8] J. P. Biersack and L. G. Haggmark, unpublished. We are grateful to the authors for making this program available to us prior to publication.

[9] K. L. Merkle, in Proceedings of the International Conference on Solid State Physics Research with Accelerators, Brookhaven National Laboratory, 1967, Report No. BNL-50083, C52, p. 359 (unpublished).

[10] H. H. Andersen and H. Sorensen, Rad. Eff. 14, (1972) 49.

[11] J. Lindhard and M. Scharff, Phys. Rev. 124, (1961) 128.

[12] H. Bethe, Ann. Phys. 5 (1930) 325.

[13] K.H. Ecker and K. L. Merkle, Phys. Rev. B18 (1978) 1020.